Class II phosphoinositide 3-kinase defines a novel signaling pathway in cell migration

Tania Maffucci,[1] Frank T. Cooke,[2] Fiona M. Foster,[3] Colin J. Traer,[3] Michael J. Fry,[3] and Marco Falasca[1]

[1]Department of Medicine, The Sackler Institute, University College London, London WC1E 6JJ, England, UK
[2]Department of Biochemistry and Molecular Biology, University College London, London WC1E 6BT, England, UK
[3]School of Animal and Microbial Sciences, University of Reading, Whiteknights, Reading RG6 6AJ, England, UK

The lipid products of phosphoinositide 3-kinase (PI3K) are involved in many cellular responses such as proliferation, migration, and survival. Disregulation of PI3K-activated pathways is implicated in different diseases including cancer and diabetes. Among the three classes of PI3Ks, class I is the best characterized, whereas class II has received increasing attention only recently and the precise role of these isoforms is unclear. Similarly, the role of phosphatidylinositol-3-phosphate (PtdIns-3-P) as an intracellular second messenger is only just beginning to be appreciated. Here, we show that lysophosphatidic acid (LPA) stimulates the production of PtdIns-3-P through activation of a class II PI3K (PI3K-C2β). Both PtdIns-3-P and PI3K-C2β are involved in LPA-mediated cell migration. This study is the first identification of PtdIns-3-P and PI3K-C2β as downstream effectors in LPA signaling and demonstration of an intracellular role for a class II PI3K. Defining this novel PI3K-C2β–PtdIns-3-P signaling pathway may help clarify the process of cell migration and may shed new light on PI3K-mediated intracellular events.

Introduction

Over the last few years, the intracellular role of phosphoinositide 3-kinases (PI3Ks), the family of enzymes responsible for generation of 3-phosphorylated phosphoinositides, has been extensively investigated and it is now established that PI3Ks are crucial components of many signaling pathways playing a pivotal role in many different physiological events (Rameh and Cantley, 1999; Cantley, 2002). Furthermore, it is also well documented that altered PI3K-dependent pathways are implicated in different diseases including cancer and diabetes (Katso et al., 2001). Although different PI3Ks have been identified and grouped into three classes (Foster et al., 2003), the majority of these studies focused on members of class I and their main in vivo product phosphatidylinositol-3,4,5-trisphosphate (PtdIns-3,4,5-P_3).

Recently, a growing interest has arisen in the members of class II PI3K and several lines of evidence suggest a potential role for these enzymes in agonist-mediated regulation of cellular functions (Foster et al., 2003). Such evidence includes activation of PI3K-C2α by insulin (Brown et al., 1999) and monocyte chemotactic peptide-1 (Turner et al., 1998) and through interaction with clathrin (Gaidarov et al., 2001). Similarly, insulin (Brown and Shepherd, 2001) and platelet aggregation (Zhang et al., 1998) have been reported to activate PI3K-C2β. In addition, PI3K-C2α and PI3K-C2β associate with polypeptide growth factor receptors (Arcaro et al., 2000) and recent data suggest that PI3K-C2β is involved in EGF- and stem cell factor–dependent signals (Arcaro et al., 2002). Despite this evidence, a clear mechanism of activation and the precise intracellular roles of these enzymes are still not defined (Foster et al., 2003). Furthermore, there is currently no clear indication of their in vivo lipid products (Foster et al., 2003), although the observation that, in vitro, these enzymes display a strong substrate preference for phosphatidylinositol suggests phosphatidylinositol-3-phosphate (PtdIns-3-P) to be their main lipid product in vivo (Brown and Shepherd, 2001).

The role of PtdIns-3-P as a dynamic intracellular second messenger has been recently underscored by our work reporting that this phosphoinositide is generated upon insulin stimulation (Maffucci et al., 2003) and the demonstration that it plays a crucial role in insulin signaling (Chaussade et al., 2003; Maffucci et al., 2003). Evidence suggests that the insulin-dependent pool of PtdIns-3-P might be generated through activation of a class II PI3K enzyme (Maffucci et al., 2003).

Lysophosphatidic acid (LPA; 1-acyl-*sn*-glycerol-3-phosphate) is a serum-borne phospholipid that evokes a wide range of biological effects, including cell proliferation, migration,

Correspondence to Marco Falasca: m.falasca@ucl.ac.uk

Abbreviations used in this paper: LPA, lysophosphatidic acid; PI3K, phosphoinositide 3-kinase; PLC, phospholipase C; PtdIns-3,4,5-P_3, phosphatidylinositol-3,4,5-trisphosphate; PtdIns-3-P, phosphatidylinositol-3-phosphate.

The online version of this article includes supplemental material.

The Journal of Cell Biology, Vol. 169, No. 5, June 6, 2005 789–799
http://www.jcb.org/cgi/doi/10.1083/jcb.200408005

and survival (Moolenaar, 1994; Graler and Goetzl, 2002; Mills and Moolenaar, 2003; van Leeuwen et al., 2003). This large spectrum of biological activities is explained by the fact that LPA receptors can couple to three distinct G proteins, Gq, Gi, and $G_{12/13}$, leading to activation of several intracellular messengers, including phospholipase C (PLC), the small GTPases RhoA and Rac, the Ras–MAPK cascade, and PI3K (Radeff-Huang et al., 2004). Two members of class I PI3K (p110β and p110γ) have been reported to be involved in LPA signaling (Yart et al., 2002). In particular, p110γ can be directly activated by G protein βγ subunits through association with the adaptor protein p101 (Stephens et al., 1997) and it has been implicated in the LPA-dependent Ras–MAPK activation (Takeda et al., 1999) and motility (Jung et al., 2004). Furthermore, it has been shown that at least in some cell lines the LPA-dependent accumulation of PI3K products is mediated by p110β in a mechanism involving transactivation of the EGF receptor (Laffargue et al., 1999).

Among the different effects elicited by LPA, migration has recently received increasing attention (Gschwind et al., 2003; Stahle et al., 2003; van Leeuwen et al., 2003; Yamada et al., 2004). The importance of LPA in migration has been underscored by the discovery that autotaxin, a cell motility-stimulating ectophosphodiesterase involved in tumor invasion, can act as a lysophospholipase D and generate LPA from lysophosphatidylcholine in the extracellular environment (Umezu-Goto et al., 2002). Indeed, both LPA and autotaxin have been involved in motility of neoplastic and nonneoplastic cells (Hama et al., 2004). Cell migration is the result of different and well-coordinated physical processes and orchestrates embryonic morphogenesis, contributes to tissue repair and regeneration, and drives disease progression in cancer, atherosclerosis, and arthritis. Several lines of evidence suggest that 3-phosphoinositides play a role in directed migration via both G protein– and tyrosine kinase–mediated signaling processes. Here, we identify a novel pathway in LPA signaling that involves generation of the lipid second messenger PtdIns-3-P through activation of PI3K-C2β and is crucial for LPA-dependent cell migration. This study is the first demonstration of an intracellular role for a class II PI3K and identification of two new important players in cell migration.

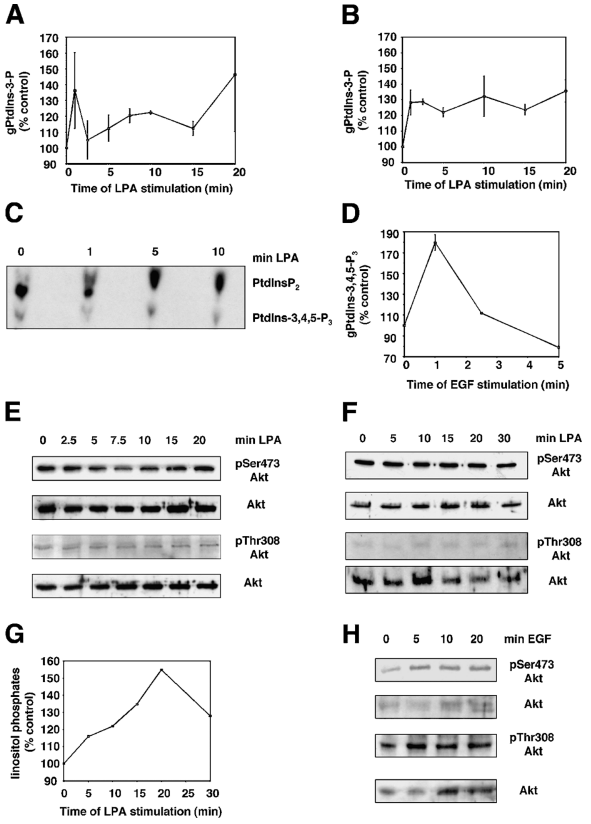

Figure 1. **LPA generates specifically PtdIns-3-P in HeLa and SKOV-3.** HeLa (A) and SKOV-3 (B) were labeled with [^{3}H]-*myo*-inositol for 24 h and stimulated with 25 μM LPA for the indicated times. Phospholipids were then extracted, deacylated, and analyzed by HPLC. Levels of PtdIns-3-P are shown as a percentage of basal levels. Data are mean ± SEM of three to four (HeLa) and three to eight (SKOV-3) independent experiments. (C) Serum-starved HeLa were labeled with [^{32}P]phosphoric acid for 3 h and stimulated with 25 μM LPA for the indicated times. Phospholipids were then extracted and analyzed by TLC. (D) Levels of PtdIns-3,4,5-P_3 in ^{3}H-labeled HeLa assessed at different times of EGF stimulation by HPLC analysis. Data are mean ± SEM of three independent experiments. (E) Western blotting analysis of lysates from serum-starved HeLa stimulated with 25 μM LPA for the indicated times. Phosphorylation of Akt on residue Ser473 and Thr308 was assessed by using specific antibodies. Filters were stripped and reprobed with an anti-Akt antibody. (F) Western blotting analysis of lysates from serum-starved SKOV-3 stimulated with 25 μM LPA for the indicated times. Phosphorylation of Akt and total Akt levels were assessed by using specific antibodies. (G) LPA-dependent activation of PLC was assessed by monitoring the levels of total inositol phosphates generated. Data are from the experiment performed in parallel with the experiment shown in F. (H) Western blotting analysis of lysates from serum-starved SKOV-3 stimulated with 20 ng/ml EGF for the indicated times. Phosphorylation of Akt and total Akt levels were assessed by using specific antibodies.

Results

LPA generates the intracellular second messenger PtdIns-3-P

We have recently demonstrated for the first time that PtdIns-3-P can act as a lipid second messenger and plays a crucial role in insulin signaling (Maffucci et al., 2003). This observation, together with our previous work reporting that LPA can generate PtdIns-3-P in COS7 cells (Razzini et al., 2000), prompted us to further investigate the effects of LPA stimulation on the levels of the PI3K products in different cell lines. HPLC analysis revealed that LPA stimulated the production of PtdIns-3-P in ^{3}H-labeled COS7 (Fig. S1, A and B, available at http://www.jcb.org/cgi/content/full/jcb.200408005/DC1), HeLa cells (Fig. 1 A), and an ovarian cancer cell line (SKOV-3; Fig. 1 B). It is important to underline that resting mammalian cells contain high basal levels of PtdIns-3-P (Rameh and Cantley, 1999); therefore, the apparent small increase upon LPA stimulation actually corresponds to a large amount of this phosphoinositide being generated de novo.

When we analyzed PtdIns-3,4,5-P_3, we observed that the levels of this phosphoinositide were very low in resting COS7 but rapidly increased upon LPA stimulation (Fig. S1 C), as reported previously (Laffargue et al., 1999). In contrast, HPLC analysis of ^{3}H-labeled cells revealed that both SKOV-3 (Fig. S2 A, available at http://www.jcb.org/cgi/

content/full/jcb.200408005/DC1) and HeLa (unpublished data) possessed high basal levels of PtdIns-3,4,5-P_3 that were unaffected by LPA stimulation. As an alternative method to detect and visualize PtdIns-3,4,5-P_3, phospholipids were extracted from ^{32}P-labeled cells and analyzed by TLC. Stimulation with LPA for different times did not increase the basal levels of PtdIns-3,4,5-P_3 in HeLa (Fig. 1 C). However, a clear increase in PtdIns-3,4,5-P_3 was observed in HeLa upon EGF stimulation in experiments performed in parallel (HPLC analysis of ^{3}H-labeled cells: Fig. 1 D; TLC analysis of ^{32}P-labeled cells: see Fig. 3 C). We checked the phosphorylation state of the well-established PtdIns-3,4,5-P_3 target protein kinase B/Akt. As a consequence of the observed high basal levels of PtdIns-3,4,5-P_3, phosphorylation of Akt was already detectable in unstimulated HeLa (Fig. 1 E) and SKOV-3 (Fig. 1, F and H). LPA stimulation for different times did not induce a further phosphorylation of Akt in either cell line (Fig. 1, E and F). Efficiency of LPA in stimulating these cells was confirmed by monitoring PLC activation in parallel experiments (Fig. 1 G, representative example of PLC activation in SKOV-3 in the experiment performed in parallel to the experiment shown in Fig. 1 F). The possibility that Akt was already maximally activated in these cells and therefore could not be further stimulated was ruled out by the observation that EGF induced a clear increase in phosphorylation of Akt in SKOV-3 (Fig. 1 H) as previously reported (Anderson et al., 2001). Similar results were obtained in HeLa (unpublished data). Together, these results indicate that LPA specifically stimulates PtdIns-3-P synthesis without detectably affecting the levels of PtdIns-3,4,5-P_3 at least in HeLa and SKOV-3.

The LPA-dependent pool of PtdIns-3-P is generated at the plasma membrane

To localize the LPA-dependent pool of PtdIns-3-P, cells were transfected with a cDNA encoding GFP-2XFYVE^{Hrs}, a GFP fusion protein known to specifically bind PtdIns-3-P (Gillooly et al., 2000; Maffucci et al., 2003). Confocal microscopy analysis revealed that in COS7 (Fig. S1 D), HeLa (Fig. 2 A), and SKOV-3 (Fig. 2 B), LPA stimulation induced a rapid translocation of GFP-2XFYVE^{Hrs} to the plasma membrane that paralleled the time course of PtdIns-3-P formation observed by HPLC analysis (for COS7 compare Fig. S1 B and histogram in Fig. S1 D; for SKOV-3 compare Fig. 1 B and Fig. S2 B). As shown in Fig. 2 C, plasma membrane translocation in SKOV-3 was confirmed by colocalization of YFP-2XFYVE^{Hrs} and the plasma membrane marker CFP-PH PLCδ1 (Maffucci et al., 2003).

To investigate the involvement of PI3K in generation of the LPA-dependent pool of PtdIns-3-P, we performed HPLC analysis in ^{3}H-labeled SKOV-3 pretreated with different concentrations of the reversible PI3K inhibitor LY294002 before stimulation with LPA. Pretreatment with LY294002 up to 10 μM did not inhibit the LPA-mediated formation of PtdIns-3-P (Fig. 3 A), although it efficiently reduced the basal levels of PtdIns-3,4,5-P_3 (unpublished data) and inhibited the basal phosphorylation of Akt (Fig. 3 B). Furthermore, TLC analysis revealed that 10 μM LY294002 completely blocked the EGF-induced generation of PtdIns-3,4,5-P_3 in SKOV-3 and HeLa

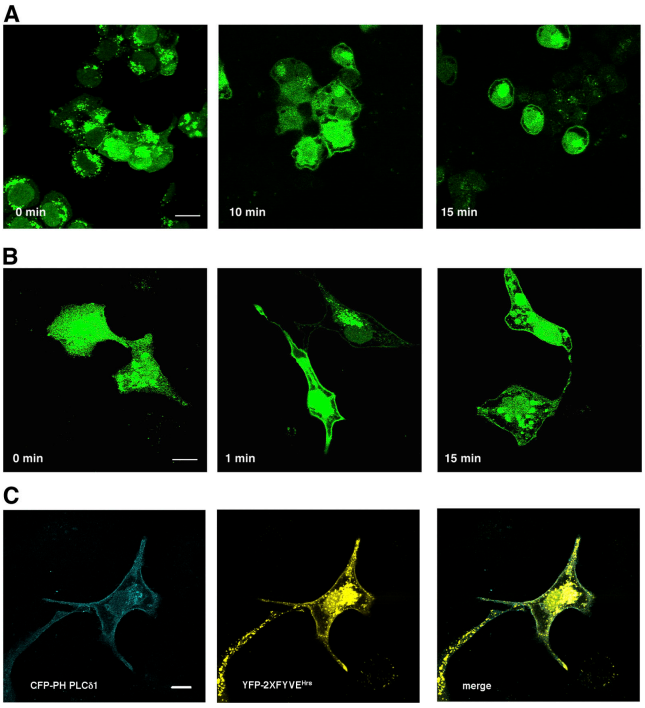

Figure 2. **The LPA-dependent pool of PtdIns-3-P is generated at the plasma membrane of HeLa and SKOV-3.** HeLa (A) and SKOV-3 (B) were transfected with a cDNA encoding GFP-2XFYVE^{Hrs}. After 24 h, cells were serum deprived and stimulated with 25 μM LPA for the indicated times before fixing for confocal microscopy analysis. (C) Confocal microscopy analysis of SKOV-3 transfected with cDNAs encoding YFP-2XFYVE^{Hrs} and CFP-PH PLCδ1 and stimulated with 25 μM LPA for 10 min. Bars, 10 μm.

(Fig. 3 C). Similarly, pretreatment with 100 nM of the irreversible PI3K inhibitor wortmannin inhibited the LPA-induced translocation of the PtdIns-3-P fluorescent probe GFP-2XFYVE^{Hrs} to the plasma membrane, whereas 10 μM LY294002 had almost no effect (Fig. 3, D and E). These data indicate that LPA generates PtdIns-3-P at the plasma membrane of COS7, HeLa, and SKOV-3 in a mechanism sensitive to wortmannin but, unlike agonist-induced PtdIns-3,4,5-P_3 production, more resistant to LY294002.

The LPA-dependent pool of PtdIns-3-P is involved in cell migration

To gain further insight into the LPA signaling in HeLa and SKOV-3 and precisely assess the role of the LPA-stimulated pool of PtdIns-3-P, we tested the effects of LPA on cell proliferation and migration in both cell lines. LPA had only a small effect on cell proliferation in HeLa, whereas it clearly increased cell growth in SKOV-3 (Fig. S3 A, available at http://www.jcb.org/cgi/content/full/jcb.200408005/DC1). In contrast, LPA induced migration in both cell lines as assessed by wound healing (Fig. 4 A; Fig. 5 A; and Fig. S3, B and C) and Transwell (Fig. 4 C, Fig. 5 C, and Fig. S3 D) assays. Therefore, we hypothesized that PtdIns-3-P might be involved in the LPA-mediated cell motility.

Effect of PI3K inhibitors. To check this hypothesis, we first tested the effect of different concentrations of PI3K inhibitors on cell migration. Wound healing assay

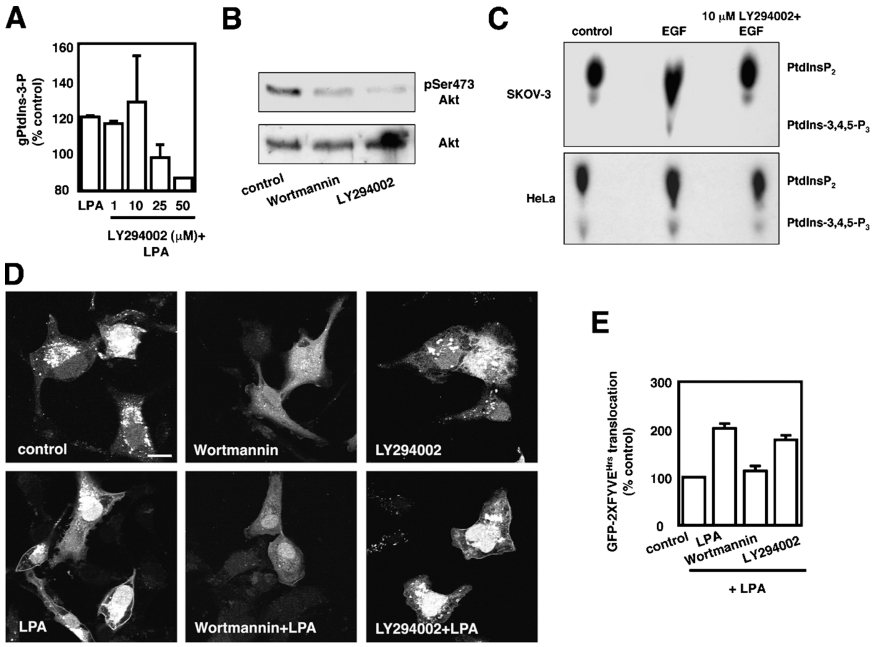

Figure 3. **Effect of PI3K inhibitors on the LPA-mediated PtdIns-3-P formation.** (A) SKOV-3 were labeled with [^{3}H]-*myo*-inositol for 24 h and left untreated or pretreated with the indicated concentrations of LY294002 before stimulation with 25 μM LPA for 10 min. Phospholipids were then extracted, deacylated, and analyzed by HPLC. Levels of PtdIns-3-P are shown as a percentage of basal levels. (B) Western blotting analysis of lysates from serum-starved SKOV-3 treated with 100 nM wortmannin or 10 μM LY294002 for 30 min. Phosphorylation of Akt on residue Ser473 was assessed by using a specific antibody. Filter was stripped and reprobed with an anti-Akt antibody. (C) SKOV-3 (top) and HeLa (bottom) were labeled with [^{32}P]phosphoric acid for 3 h and left untreated or pretreated with 10 μM LY294002 before stimulation with 20 ng/ml EGF for 5 (SKOV-3) or 1 min (HeLa). Phospholipids were extracted and analyzed by TLC. (D) GFP-2XFYVE^{Hrs}-expressing SKOV-3 cells were pretreated with 100 nM wortmannin or 10 μM LY294002. After 30 min, cells were stimulated with 25 μM LPA for 10 min before fixing for confocal microscopy analysis. Bar, 10 μm. (E) Quantitative analysis of experiments as in D. Data are mean ± SEM of five independent experiments.

monitored by time-lapse microscopy (Fig. 4, A and B) and Transwell assay (Fig. 4 C) indicated that a pretreatment with wortmannin inhibited the LPA-dependent migration. In contrast, a concentration of 1 μM LY294002 did not affect the LPA-dependent migration (Fig. 5, A and B) and 10 μM LY294002 had only a partial inhibitory effect (Fig. 5, A and B, wound healing assay monitored by time-lapse microscopy; Fig. 5 C, Transwell assay). Together, these data indicate that generation of the LPA-dependent pool of PtdIns-3-P and the LPA-induced migration show a similar sensitivity to PI3K inhibitors.

Effect of PtdIns-3-P–specific phosphatase.

These observations further prompted us to specifically check a potential role for PtdIns-3-P in LPA-dependent migration. Therefore, we analyzed migration of SKOV-3 transfected with a cDNA encoding a Flag-tagged PtdIns-3-P–specific phospha-

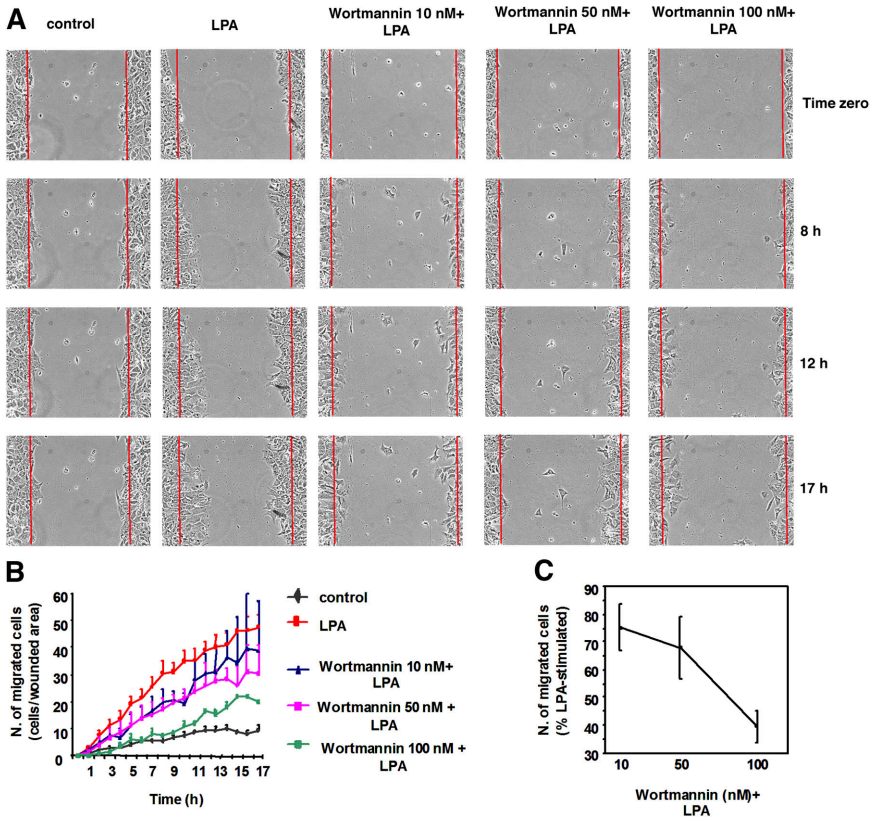

Figure 4. **Effect of wortmannin on the LPA-mediated migration.** (A and B) Time-lapse microscopy of wound healing assay in SKOV-3 pretreated with the indicated concentrations of wortmannin for 30 min. Images in A show the wounded cell monolayers at time 0 and after the indicated hours in the absence (control) or presence of 25 μM LPA with or without the inhibitor. (B) Quantitative analysis was performed as described in Materials and methods. Data are mean ± SEM of three to four independent experiments. (C) Serum-starved SKOV-3 were pretreated with the indicated concentrations of wortmannin for 30 min. Migration was assessed by Transwell assay in the presence of 25 μM LPA and the indicated concentrations of the inhibitor. Data are mean ± SEM of five independent experiments and are expressed as a percentage of LPA-stimulated cells. In these experiments, LPA induced a three- to fourfold increase in cell migration.

tase, myotubularin MTM1 (Laporte et al., 2002), that has been recently successfully used to inhibit the insulin-dependent pool of PtdIns-3-P (Chaussade et al., 2003). In these experiments, migration was assessed in Transwell assays by counting the total number of migrated cells as described in Materials and methods. Although the transfection efficiency in SKOV-3 was only ~50%, overexpression of MTM1 was able to reduce the LPA-induced migration whereas overexpression of the point mutant MTM1 C375S, which has no phosphatase activity toward PtdIns-3-P, had no effect (Fig. 6 A, top). Expression of both proteins was assessed in Western blotting analysis (Fig. 6 A, bottom). Although expression of MTM1 was able to induce a partial inhibition of migration, it did not seem to affect the levels of PtdIns-3,4,5-P_3 as basal Akt phosphorylation was not even partially reduced (Fig. 6 B). Importantly, the lack of effect on Akt phosphorylation was not due to the transfection efficiency because overexpression of the PtdIns-3,4,5-P_3–specific phosphatase PTEN at similar transfection efficiency was indeed able to reduce Akt phosphorylation (Fig. 6 C).

Effect of PtdIns-3-P-specific binding domains. We analyzed the LPA-dependent migration in cells overexpressing the GFP-2XFYVE^{Hrs} fusion protein that we hypothesized might act as a PtdIns-3-P–sequestering domain and therefore interfere with the LPA-dependent pool of PtdIns-3-P. Wound healing assays monitored by confocal microscopy revealed that overexpression of GFP-2XFYVE^{Hrs} inhibited the LPA-dependent migration in SKOV-3, whereas overexpression of GFP alone had no effect (Fig. 6 D). Because none of the GFP-2XFYVE^{Hrs}-transfected cells were able to migrate into the wounded area, we could not perform a quantitative analysis of this assay (Fig. 6 D). Therefore, to quantify the effect of overexpression of the PtdIns-3-P–binding domain, we transfected cells with cDNAs encoding GFP alone or GFP-2XFYVE^{Hrs} and analyzed migration by using Transwell assays. In a first set of experiments, we counted the total number of cells migrated after staining the membranes of the Transwell chambers with crystal violet and we observed that LPA clearly stimulated migration in GFP-transfected cells, whereas overexpression of GFP-2XFYVE^{Hrs} partially reduced the LPA-dependent migration (Fig. 6 E). The observed partial effect was consistent with a transfection efficiency of ~50%, as discussed in the previous paragraph.

To clearly assess the effect of the PtdIns-3-P–sequestering domain, we performed a very accurate second set of experiments and counted only the transfected (green) cells that had migrated. Indeed, in this more precise assay we observed that migration was completely inhibited in cells expressing GFP-2XFYVE^{Hrs}, whereas cells expressing GFP alone migrated upon LPA stimulation (Fig. 6 F). As discussed in the previous section, although a 50% transfection efficiency of GFP-PTEN was enough to reduce Akt phosphorylation, basal levels of Akt phosphorylation were not even partially reduced in cells transfected with GFP-2XFYVE^{Hrs} with the same efficiency (Fig. 6 G).

When we performed similar experiments in HeLa we observed a total inhibition of the LPA-mediated migration in cells expressing GFP-2XFYVE^{Hrs}, a finding consistent with the high transfection efficiency of these cells (>80%; Fig. 6, H and I; and Fig. S3 E). To further confirm that inhibition of migration was due to a specific sequestering of PtdIns-3-P, we transfected

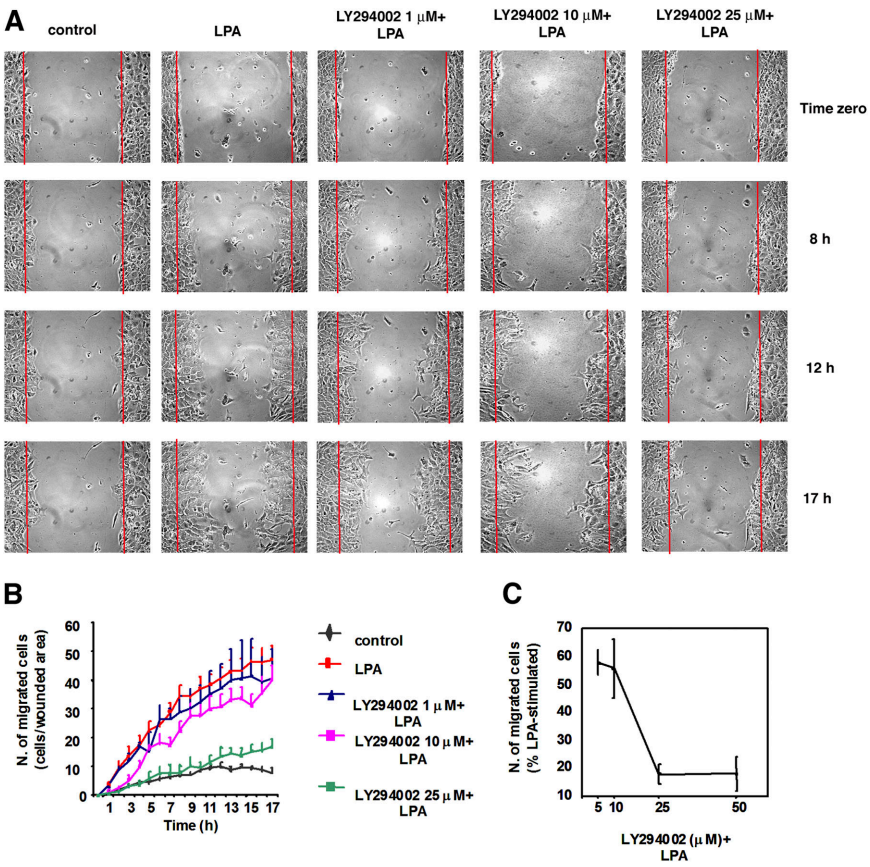

Figure 5. **Effect of LY294002 on the LPA-mediated migration.** (A and B) Time-lapse microscopy of wound healing assay in SKOV-3 pretreated with the indicated concentrations of LY294002 for 30 min. Images in A show the wounded cell monolayers at time 0 and after the indicated hours in the absence (control) or presence of 25 μM LPA with or without the inhibitor. (B) Quantitative analysis was performed as described in Materials and methods. Data are mean ± SEM of three to five independent experiments. (C) Serum-starved SKOV-3 were pretreated with the indicated concentrations of LY294002 for 30 min. Migration was assessed by Transwell assay in the presence of 25 μM LPA and the indicated concentrations of the inhibitor. Data are mean ± SEM of five independent experiments and are expressed as a percentage of LPA-stimulated cells. In these experiments, LPA induced a three- to fourfold increase in cell migration.

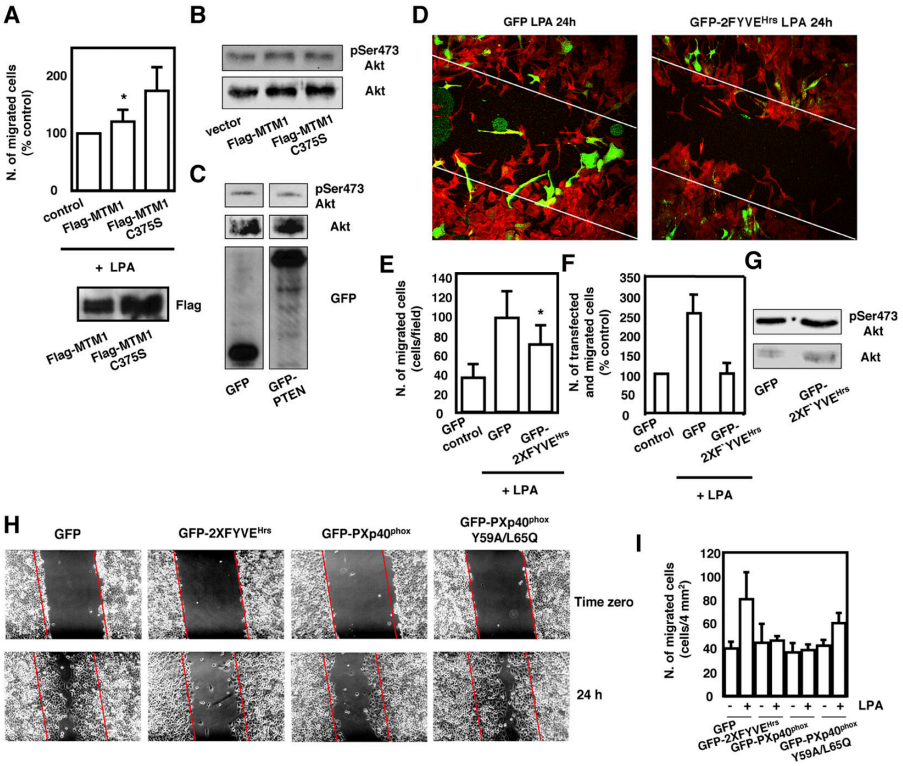

Figure 6. **PtdIns-3-P is involved in the LPA-mediated migration of SKOV-3.** (A-G) SKOV-3 were transiently transfected with the indicated cDNAs. Transfection efficiency in these cells was ~50%. (A, top) SKOV-3 were transfected with cDNAs encoding Flag-MTM1 and Flag-MTM1 C375S. After 24 h, cells were serum deprived overnight and migration was assessed by Transwell assay in the presence of 25 μM LPA. The total number of migrated cells was counted after staining the membranes of the Transwell chambers with crystal violet. Data are mean ± SEM of three independent experiments. *, $P < 0.05$. (bottom) Representative blot monitoring the levels of expression of Flag-MTM1 and Flag-MTM1 C375S by using an anti-Flag antibody. (B) Phosphorylation of Akt on residue Ser473 assessed in lysates from SKOV-3 transfected with an empty vector or cDNAs encoding Flag-MTM1 and Flag-MTM1 C375S. Filters were stripped and reprobed with an anti-Akt antibody. (C) Phosphorylation of Akt on residue Ser473 assessed in lysates from SKOV-3 transfected with cDNAs encoding GFP or GFP-PTEN. Filters were stripped and reprobed with an anti-Akt antibody. Expression of the exogenous proteins was assessed by using an anti-GFP antibody. Images are from different lanes in the same blot. (D) SKOV-3 grown on glass coverslips were transfected with cDNAs encoding GFP or GFP-2XFYVE^{Hrs}. After 24 h, cells were serum deprived overnight and migration was assessed by wound healing assay. After wounding and further 24 h in the presence of 25 μM LPA, cells were fixed and analyzed by confocal microscopy. Actin was stained by using Alexa 594 phalloidin and the merged images are shown. Diagonal lines specify the position of the original wound. (E and F) SKOV-3 were transfected as in D. Migration was then assessed by Transwell assay in the presence of 25 μM LPA. For data shown in E, the total number of cells that had migrated was counted after staining the membranes of the Transwell chambers with crystal violet. Data are mean ± SEM from three independent experiments performed in duplicate. *, $P < 0.05$. For data shown in F, the membranes of the Transwell chambers were fixed and analyzed by fluorescent microscopy to visualize and count only transfected (green) cells that had migrated. Data are mean ± SEM from four independent experiments. (G) Phosphorylation of Akt on residue Ser473 assessed in lysates from SKOV-3 transfected with cDNAs encoding GFP or GFP-2XFYVE^{Hrs}. Filters were stripped and reprobed with an anti-Akt antibody. (H–I) HeLa were transfected with cDNAs encoding the indicated fusion proteins (transfection efficiency was >80%). After 24 h, cells were serum deprived overnight and wound healing was performed in the presence of 25 μM LPA. (H) Representative phase-contrast images of the wounded cell monolayers at time 0 and after 24 h of migration. (I) Quantitative analysis of wound healing as in H. Data are mean ± SEM of three independent experiments.

HeLa with a cDNA encoding another fusion protein also known to bind PtdIns-3-P (GFP-PX p40^{phox}) that we have already used to monitor the intracellular PtdIns-3-P (Maffucci et al., 2003). As a control we used a mutant of this domain with a reduced ability to bind PtdIns-3-P (GFP-PX p40^{phox} Y59A/L65Q). GFP-PX p40^{phox} inhibited the LPA-mediated migration, whereas less effect was observed in cells transfected with the mutated version of the protein (Fig. 6, H and I). Similar results were obtained in Transwell assay (Fig. S3 E). Overexpression of these domains did not affect cell growth (Fig. S3 F).

Together these data indicate that the lipid second messenger PtdIns-3-P is a new effector in LPA cascade and plays a role in the LPA-mediated cell migration.

The LPA-dependent pool of PtdIns-3-P is generated through PI3K-C2β activation

The observation that in HeLa and SKOV-3 LPA did not affect the levels of PtdIns-3,4,5-P_3, the major in vivo product of class I PI3Ks, together with the observed resistance to the inhibitor LY294002 ruled out the possibility that PtdIns-3-P derives from activation of the class I PI3Ks. This finding is in agreement with recent data indicating that the LPA-dependent migration of SKOV-3 requires activation of a Ras–MEK kinase 1 pathway but not class I PI3K (Bian et al., 2004). Several lines of evidence suggest that, at least in insulin signaling, the stimulated pool of PtdIns-3-P is the product of a class II PI3K (Maffucci et al., 2003). Moreover, the high sensitivity to wortmannin and reduced sensitivity to LY294002 observed in this study was in agreement with observed in vitro sensitivities of the class II enzyme PI3K-C2β to these inhibitors and is distinct from that observed for class I enzymes (Arcaro et al., 1998; Fig. S4, A and B, available at http://www.jcb.org/cgi/content/full/jcb.200408005/DC1). On the basis of these observations, we hypothesized that the LPA-dependent pool of PtdIns-3-P might be generated through activation of a class II PI3K.

To investigate this hypothesis, we examined the effect of specific inhibition of these isoforms on the LPA-dependent generation of PtdIns-3-P at the plasma membrane. As there are no class II PI3K-specific chemical inhibitors available, we used RNA interference to specifically knockdown the class II isoforms PI3K-C2β and PI3K-C2α. Then, we analyzed the intracellular localization of GFP-2XFYVE^{Hrs} in LPA-stimulated SKOV-3 transfected with the corresponding siRNAs. A complete inhibition of LPA-dependent GFP-2XFYVE^{Hrs} plasma

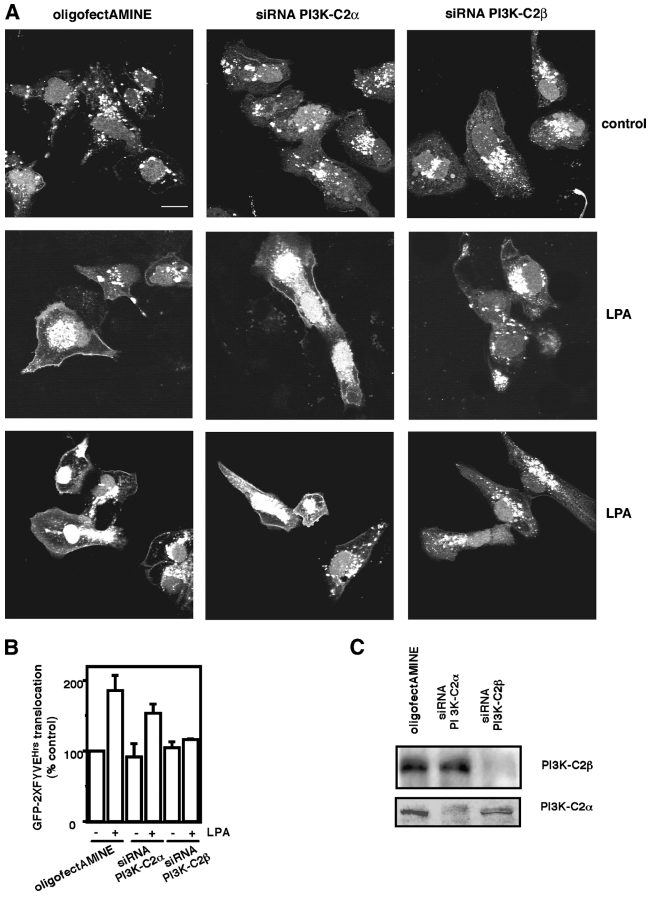

Figure 7. **Knockdown of PI3K-C2β completely inhibits the LPA-mediated PtdIns-3-P formation.** (A) SKOV-3 were transfected with oligofectAMINE alone or with siRNAs corresponding to PI3K-C2α and PI3K-C2β and further transfected with a cDNA encoding GFP-2XFYVE^{Hrs}. After 24 h, cells were serum deprived overnight and stimulated with 25 μM LPA for 10 min before fixing for confocal microscopy analysis. Bar, 10 μm. (B) Quantitative analysis of GFP-2XFYVE^{Hrs} translocation to the plasma membrane in SKOV-3 as in A. Data are mean ± SEM from three independent experiments. (C) Representative blots of lysates from SKOV-3 transfected with oligofectAMINE or the indicated siRNAs. Levels of PI3K-C2α and PI3K-C2β were assessed by using specific antibodies.

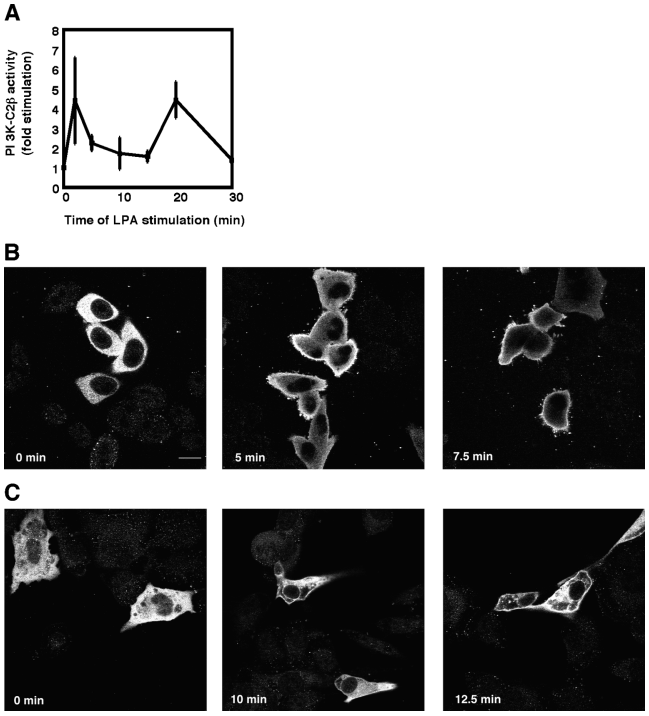

Figure 8. **PI3K-C2β is a downstream effector of LPA.** (A) PI3K-C2β activity was assessed in LPA-stimulated HeLa by in vitro kinase assay as described in Materials and methods. Data are mean ± SEM of three independent experiments. (B and C) HeLa (B) and SKOV-3 (C) were transfected with a cDNA encoding a myc-tagged PI3K-C2β. After 24 h, cells were serum deprived overnight and stimulated with 25 μM LPA for the indicated times before fixing for confocal microscopy analysis. Bar, 10 μm.

membrane translocation was observed in SKOV-3 transfected with the PI3K-C2β siRNA. No inhibition was observed in cells transfected with the PI3K-C2α siRNA (Fig. 7, A and B). The observed complete inhibition was consistent with a high uptake of siRNAs in SKOV-3 that was confirmed by Western blotting analysis showing that a >90% knockdown of protein expression was achieved (Fig. 7 C). The higher transfection efficiency compared with plasmid DNAs is in agreement with reported high uptake of siRNAs in cells (Holen et al., 2002; Splinter et al., 2003). The LPA-dependent activation of PI3K-C2β was confirmed by in vitro lipid kinase assay (Fig. 8 A). In the same experiments, no activation of PI3K-C2α was observed (unpublished data). In addition, we observed that LPA induced the translocation of a myc-tagged version of PI3K-C2β to the plasma membrane in both HeLa (Fig. 8 B) and SKOV-3 (Fig. 8 C), suggesting that formation of PtdIns-3-P might occur through an LPA-dependent targeting and subsequent activation of the enzyme at the plasma membrane.

PI3K-C2β is necessary for LPA-dependent migration

We investigated the potential role of class II PI3Ks in the LPA-mediated cell migration by performing migration assays on cells transfected with the isoform-specific siRNAs. Wound healing assay monitored by time-lapse microscopy revealed that knockdown of PI3K-C2β expression inhibited cell migration in SKOV-3 (Fig. 9 A). Similar results were obtained in wound healing assay performed in HeLa (Fig. S4 C). In both cases no effect was observed in cells transfected with the PI3K-C2α siRNA. Similarly, knockdown of PI3K-C2β expression completely inhibited cell migration assessed by Transwell assay both in SKOV-3 (Fig. 9 B) and HeLa (Fig. 9 C). Representative fields of migrated HeLa in Transwell assay are shown in Fig. 9 D. The complete inhibition of migration was consistent with the high uptake of siRNAs in these cells (Western blotting analysis for HeLa is shown in Fig. S4 D). These data indicate that PI3K-C2β plays an important role in the LPA-dependent migration.

Discussion

LPA activates the class II enzyme PI3K-C2β and generates the lipid second messenger PtdIns-3-P

A role for PtdIns-3-P as an intracellular second messenger has been suggested by the recent demonstration that this phosphoinositide plays an important role in insulin signaling (Chaus-

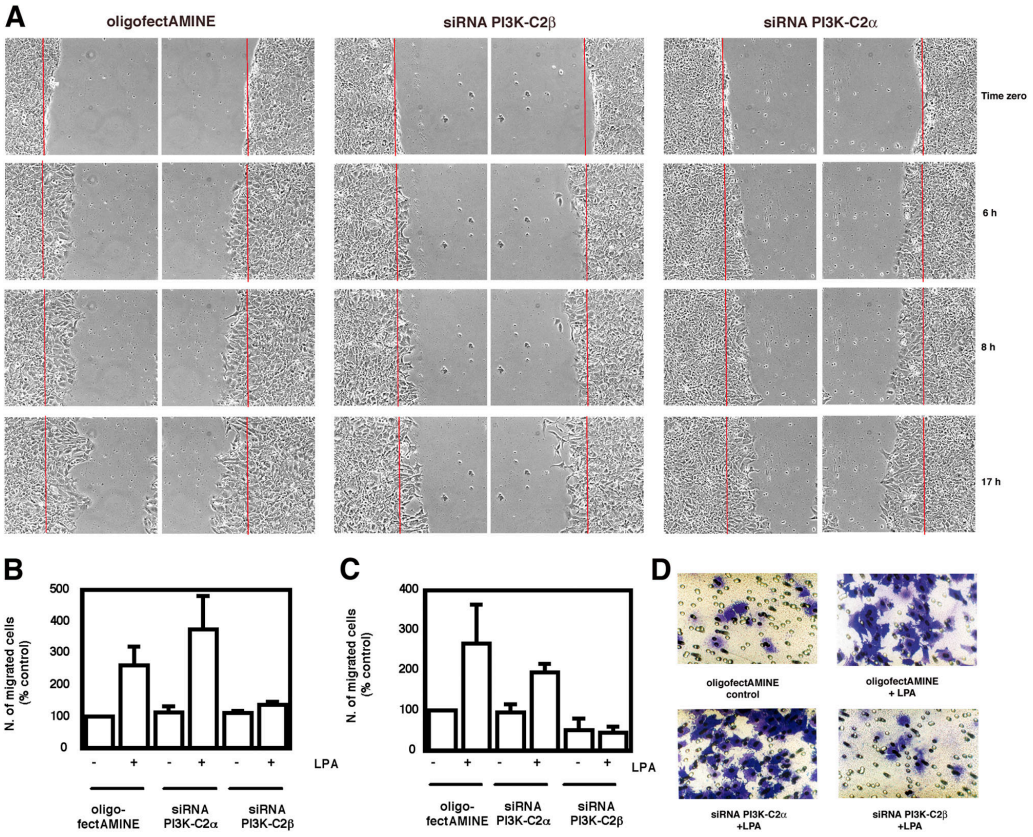

Figure 9. **PI3K-C2β is involved in LPA-mediated cell migration.** (A) Time-lapse microscopy of wound healing assay in serum-deprived SKOV-3 transfected with oligofectAMINE or the indicated siRNAs. Images show two opposite sides of the same representative fields of the recorded wounded area at time 0 and at the indicated hours in the presence of 25 μM LPA. (B) Transwell assay of serum-deprived SKOV-3 transfected with oligofectAMINE or with the indicated siRNAs. Data are mean ± SEM of four independent experiments performed in duplicate. (C) Transwell assay of serum-deprived HeLa transfected with oligofectAMINE or with the indicated siRNAs. Data are mean ± SEM of three independent experiments. (D) Representative phase-contrast images of migrated HeLa in Transwell assay as in C obtained by staining the membranes of the Transwell chambers with crystal violet.

sade et al., 2003; Maffucci et al., 2003). Here, we demonstrate that LPA can generate PtdIns-3-P at the plasma membrane of COS7, HeLa, and the ovarian cancer cell line SKOV-3, which indicates that pools of PtdIns-3-P can be generated by different stimuli and therefore PtdIns-3-P might play a more general role in signal transduction. The LPA-mediated generation of PtdIns-3-P seems to be very specific, at least in HeLa and SKOV-3, because in our experimental conditions we did not detect any formation of PtdIns-3,4,5-P_3 either by HPLC or TLC analysis. These data indicate that, at least in these cells, formation of PtdIns-3-P does not involve activation of p110γ or p110β, the members of class I PI3K most frequently associated with LPA signaling (Yart et al., 2002). Furthermore, generation of this LPA-dependent pool of PtdIns-3-P is sensitive to treatment with 100 nM of the PI3K inhibitor wortmannin but is more resistant to treatment with concentrations of LY294002 up to 10 μM, known to completely block class I PI3K. Such sensitivity to the PI3K inhibitors is consistent with observed in vitro sensitivities of the class II enzyme PI3K-C2β (Arcaro et al., 1998; Fig. S4, A and B). This observation together with our evidence suggesting that the insulin-dependent pool of PtdIns-3-P is generated through a class II PI3K-mediated mechanism led us to hypothesize that the LPA-dependent pool of PtdIns-3-P might be the product of a class II PI3K.

There is currently a growing interest in class II PI3Ks because several lines of evidence suggest that different agonists can activate these enzymes; however, their precise intracellular role and their lipid products in vivo still remain to be established (Foster et al., 2003). Here, we show that LPA activates PI3K-C2β and that knockdown of this enzyme specifically inhibits formation of PtdIns-3-P at the plasma membrane upon LPA stimulation. This is the first paper showing that PI3K-C2β is activated and PtdIns-3-P is generated upon LPA stimulation, and therefore, this work identifies a novel PI3K-C2β–PtdIns-3-P pathway in LPA signaling. Furthermore, this study is the first clear indication that PtdIns-3-P might be the in vivo product of PI3K-C2β.

The PI3K-C2β–PtdIns-3-P pathway is involved in the LPA-dependent cell migration

The observation that the sensitivity to PI3K inhibitors of LPA-dependent migration is very similar to the effect observed on PtdIns-3-P formation led us to hypothesize that this pathway might be involved in the LPA-dependent cell migration. As for PtdIns-3-P formation, treatment with 100 nM wortmannin blocked migration whereas 1 μM LY294002 had no effect and 10 μM LY294002 had a partial effect on the LPA-mediated

migration. Sensitivity to LY294002 is a key feature of PI3K-C2β that shows a different sensitivity to this inhibitor compared with class I PI3K (Fig. S4 B). In particular, 1 μM LY294002, although able to significantly inhibit class I PI3K, has no effect on the activity of PI3K-C2β. More crucially, a concentration of 10 μM LY294002 completely blocks class I PI3K, whereas it has only a partial inhibitory effect on PI3K-C2β. It is important to underline that 10 μM LY294002 represents a crucial point in the curve of sensitivity of PI3K-C2β that is where the activity of the enzyme significantly drops (Fig. S4 B). The observation that 10 μM LY294002 corresponds to the slope in the curve of sensitivity of PI3K-C2β might explain the variability in the results that in some experiments was associated with the use of such concentration of the inhibitor (e.g., see the high SEM associated with the PtdIns-3-P formation in Fig. 3 A). However, even taking into account such variability, it is clear that both the LPA-dependent generation of PtdIns-3-P and migration are quite resistant to treatment with LY294002, and this finding is consistent with the observed sensitivity of PI3K-C2β.

Specific blockade of PtdIns-3-P (by overexpression of either a PtdIns-3-P–specific phosphatase or PtdIns-3-P–binding domains) blocks the LPA-dependent migration. In SKOV-3, the observed effects were partial when we counted the total number of migrated cells, and this result is consistent with a partial transfection efficiency of plasmid DNAs in SKOV-3 (~50%). However, when we monitored migration only in transfected (green) SKOV-3, we observed a complete inhibition of migration. Similarly, inhibition of migration was complete in HeLa whose transfection efficiency was >80%. Additionally, knockdown of PI3K-C2β in both cell lines inhibits the LPA-mediated migration. Together, these data indicate that this newly identified PI3K-C2β–PtdIns-3-P signaling pathway is necessary for the LPA-dependent cell migration. These data represent the first clear identification of an intracellular role for a member of class II PI3K and they may shed new light on PI3K-mediated intracellular events.

Over the last decade wide interest has been focused on understanding the mechanisms underlying the major steps of cell migration and the signaling pathways regulating them. On the one hand, cell migration plays a crucial role in a variety of biological processes such as morphogenesis, inflammation, and wound healing. On the other hand, migration is involved in several diseases, including cancer metastasis, atherosclerosis, and arthritis. Therefore, the identification of both PI3K-C2β and PtdIns-3-P as important players in cell migration may help clarify both physiological and pathological mechanisms of cell migration and represent a novel target for therapeutic intervention. Several lines of evidence are now revealing the crucial role for LPA as a motility factor. It has been shown that in human pancreatic carcinoma cell lines LPA stimulates cell migration but not proliferation (Stahle et al., 2003). More interestingly, LPA has been identified as a critical component of ascites for the motility of pancreatic cancer cells (Yamada et al., 2004). In addition, it has been reported that the ectoenzyme autotaxin, a cell motility-stimulating ectophosphodiesterase, can generate LPA in the extracellular environment (Umezu-Goto et al., 2002), and both LPA and autotaxin are involved in motility of neoplastic and nonneoplastic cells (Hama et al., 2004). These data, together with the observation that elevated plasma LPA concentrations have been found in patients with ovarian cancer compared with healthy control group (Xu et al., 1995; Westermann et al., 1998) and that prostate cancer cells produce high levels of LPA (Xie et al., 2002), definitively support a role for LPA in the initiation or progression of malignant disease (Mills and Moolenaar, 2003).

The discovery of this novel PI3K-C2β–PtdIns-3-P pathway in LPA-dependent migration of different cell lines, including an ovarian cancer cell line, may therefore result useful in elucidating the role of LPA in this disease. Furthermore, because a wide range of mammalian cell types are LPA-responsive, it is tempting to speculate that the PI3K-C2β–PtdIns-3-P pathway might have a more general role in different biological contexts.

Materials and methods

Materials and plasmids

L-α-LPA, oleoyl (C18:1,[cis]-9), anti-myc, anti–β-actin, and anti-Flag were purchased from Sigma-Aldrich; anti-Akt, anti-pSer473Akt, and anti-pThr308 from Santa Cruz Biotechnology, Inc.; anti-HA from Boehringer; anti-p85 from Upstate Biotechnology; anti-PI3K-C2β and anti-GFP from BD Biosciences; and Alexa 594 phalloidin from Molecular Probes. Anti-PI3K-C2α was a gift of P.R. Shepherd (University of Auckland, Auckland, New Zealand). Flag-MTM1 and Flag-MTM1 C375S were a gift of J. Laporte (Institut de Génétique et de Biologie Moléculaire et Cellulaire, Illkirch, France). myc-PI3K-C2β was provided by M.D. Waterfield (The Ludwig Institute for Cancer Research, London, UK). Chemically synthesized double-stranded siRNAs with 19-nucleotide duplex RNA and 2-nucleotide 3′ dTdT overhangs were purchased from Dharmacon or Eurogentec. To design class II PI3K-specific siRNAs, the human PI3K-C2α (GenBank/EMBL/DDBJ accession no. NM 002645) and PI3K-C2β (GenBank/EMBL/DDBJ accession no. NM 002646) mRNA sequences were searched for 21-nucleotide unique sequences using the National Center for Biotechnology Information database and the BLAST search algorithm. The cDNA sequences against which siRNAs were prepared are 5′-AAGTCCAGTCACAGCGCAAAG-3′ (nucleotides 1224–1244) for PI3K-C2α and 5′-AAGAATGCGACGCCTGGCAAG-3′ (nucleotides 1368–1388) for PI3K-C2β.

Cell cultures and transfection

Cells were maintained in DME supplemented with 10% FBS and transfected with LipofectAMINE PLUS (Invitrogen) according to the manufacturer. Transfection with siRNAs was performed as described previously (Elbashir et al., 2002) and cells were used after 48–72 h.

HPLC analysis

COS7, HeLa, and SKOV-3 were incubated with 10 μCi/well *myo*-[^{3}H]inositol (PerkinElmer) in inositol-free medium M199 for 24 h, and then left untreated or stimulated with LPA for different times. HPLC analysis was performed as described previously (Maffucci et al., 2003).

TLC analysis

Serum-starved cells were incubated with 0.8 mCi/well [^{32}P]phosphoric acid (PerkinElmer) in phosphate-free medium, M3786, for 3 h before stimulation as indicated. Phospholipids were extracted, dried under nitrogen, resuspended in 100 μl chloroform/methanol (3:2), and spotted onto silica plates presoaked in water/methanol (3:2) and 1.2% (wt/vol) oxalic acid, and oven baked for 15 min at 110°C. TLC plates were developed in chloroform/acetone/methanol/acetic acid/water (90:36:30:27:18).

Confocal microscopy and quantitative analysis

Cells grown on glass coverslips were fixed with PBS containing 4% PFA for 10 min at RT. Where necessary, cells were permeabilized with 0.25% Triton X-100 and incubated with an anti-myc antibody followed by an FITC secondary antibody. Microscopy was performed by using a laser confocal microscope system (TCS NT; Leica) connected to a microscope (model DMXRE; Leica) equipped with a 63× water immersion objective. Images were acquired and loaded by using a TCS NT program (version 1.6.587).

No further processing of the images was done except for changes in brightness/contrast to better visualize the data. For quantitative analyses of GFP-2XFYVE^{Hrs} translocation, GFP-2XFYVE^{Hrs}-transfected cells were serum starved for 24 h and stimulated with LPA for the indicated times before fixing for confocal microscopy. At least 100 cells/coverslip were analyzed by blind scoring (no score: cells with 0–25% membrane localization; score 1: cells with >25% membrane localization). The number of cells showing a plasma membrane localization of the GFP-2XFYVE^{Hrs} was expressed as a percentage of control. Statistical analyses were performed by paired *t* test.

PI3K assay

PI3K activity assay was performed as described previously (Kamalati et al., 2000).

Migration assays

Wound healing assay. Confluent cells were serum deprived overnight, left untreated or treated as indicated, and then wounded with a linear scratch by a sterile pipette tip. After washing, cells were incubated in the presence or absence of LPA and 0.5 μg/ml mitomycin-C. Time-lapse microscopy was performed by using a microscope (model Eclipse TE2000-U; Nikon) equipped with a temperature controller (Solvent Scientific; 37°C). No further processing of the images was done except for changes in brightness/contrast to better visualize the data. Cell movement was recorded with a charge-coupled device camera (OrcaER; Hamamatsu Photonics) by using PCI Software (Digitalpixel). To obtain the quantitative analyses of Fig. 4 B and Fig. 5 B, panels as those shown in Fig. 4 A and Fig. 5 A were prepared for each experiment. Each panel was made up of images of cells collected at time 0 and every hour (1–17 h) for each condition (control, LPA, and different concentrations of PI3K inhibitors+LPA). The wounded area was defined in each image by positioning red lines in correspondence of the original scratch. The number of cells migrated into the wounded area at different hours was visually counted. Alternatively, the wounded cell monolayers were photographed using a microscope (Nikon). For quantitative analysis shown in Fig. 6 I, experiments were performed in cell culture dishes with a 2-mm grid (Nunc) and migration was quantified by counting the number of cells per grid square (4 mm^2) by using a microscope (Nikon).

Transwell assay. Alternatively, cell migration was performed in Transwell chambers (tissue culture treated, 10-mm-diam, 8 μm pores; Nunc) coated with 100 μg/ml of type I collagen. Cells were resuspended in DME containing 1% BSA, added (30,000 cells/150 μl) to the top of each migration chamber, and allowed to migrate in the presence of LPA in the lower chamber. After 4 h, cells that had not migrated were removed using a cotton swab, whereas migrated cells were fixed with 4% PFA. To count the total number of migrated cells, the membranes of the Transwell chambers were stained with 1% crystal violet and analyzed by phase-contrast microscopy using a microscope (Nikon; examples are shown for HeLa in Fig. 9 D). To count only the transfected cells, we took advantage of the observation that they expressed GFP-tagged proteins. Therefore, the Transwell chambers were analyzed by fluorescent microscopy using a microscope (model DM-RXE; Leica) equipped with a 10× objective. In this way, only fluorescent (green) cells that had migrated were visualized and counted.

Cell growth

10^4 cells/well in a 48-well plate were serum deprived overnight before adding LPA for a further 48 h. [^{3}H]thymidine (0.5 μCi/well) was added for the last 18 h. After washing with ice-cold PBS, wells were incubated with 5% TCA at +4°C for 20 min, washed with PBS and methanol, and air dried. After 30 min in 0.2 M NaOH, samples were collected and radioactivity was assessed by scintillation counting. Alternatively, MTT assay was performed as described previously (Piccolo et al., 2004).

Phospholipase *C* activation

Cells were incubated with 2 μCi/well *myo*-[^{3}H]inositol (PerkinElmer) in M199. After 24 h, cells were incubated in M199 plus 10 mM Hepes and 20 mM LiCl for 15 min before stimulation, scraped in 0.1 M HCOOH, and the total amount of inositol phosphates was assessed using AG 1-X8 resin (formate form, 200–400 mesh; Bio-Rad Laboratories) and liquid radioactivity counting.

Online supplemental material

Fig. S1, Fig. S2, Fig. S3, Fig. S4 and the corresponding legends are available in the online supplemental material. Online supplemental material is available at http://www.jcb.org/cgi/content/full/jcb.200408005/DC1.

We thank Professor M.A. Horton, Dr. G. Schiavo, and Professor P.R. Shepherd for critical reading of the manuscript; The Ludwig Institute for Cancer Research for the myc-tagged PI3K-C2β construct, Dr. J. Laporte for MTM1 constructs, Professor P.R. Shepherd for anti–PI3K-C2α antibody, and Mike Lau for help with the experiments in Fig. S4 (A and B).

This work was supported by the Association for International Cancer Research (grant 05-127 to M. Falasca), Compagnia di San Paolo (to M. Falasca), and Diabetes UK (grant BDA:RD02/0002388 to M. Falasca). T. Maffucci is the recipient of a Diabetes UK RD Lawrence Fellowship (grant BDA:RD04/0002884). F.T. Cooke, F.M. Foster, and C.J. Traer are supported by the Wellcome Trust, the Biotechnology and Biological Sciences Research Council (grant 4S/C14421 to M.J. Fry), and a Research Endowment Trust Funds studentship from the University of Reading, respectively. M. Falasca is supported by an endowment from the Dr. Mortimer and Mrs. Theresa Sackler Trust.

The authors declare that there are no conflicts of interest regarding this article.

Submitted: 2 August 2004
Accepted: 14 April 2005

References

Anderson, N.G., T. Ahmad, K. Chan, R. Dobson, and N.J. Bundred. 2001. ZD1839 (Iressa), a novel epidermal growth factor receptor (EGFR) tyrosine kinase inhibitor, potently inhibits the growth of EGFR-positive cancer cell lines with or without erbB2 overexpression. *Int. J. Cancer.* 94: 774–782.

Arcaro, A., S. Volinia, M.J. Zvelebil, R. Stein, S.J. Watton, M.J. Layton, I. Gout, K. Ahmadi, J. Downward, and M.D. Waterfield. 1998. Human phosphoinositide 3-kinase C2beta, the role of calcium and the C2 domain in enzyme activity. *J. Biol. Chem.* 273:33082–33090.

Arcaro, A., M.J. Zvelebil, C. Wallasch, A. Ullrich, M.D. Waterfield, and J. Domin. 2000. Class II phosphoinositide 3-kinases are downstream targets of activated polypeptide growth factor receptors. *Mol. Cell. Biol.* 20:3817–3830.

Arcaro, A., U.K. Khanzada, B. Vanhaesebroeck, T.D. Tetley, M.D. Waterfield, and M.J. Seckl. 2002. Two distinct phosphoinositide 3-kinases mediate polypeptide growth factor-stimulated PKB activation. *EMBO J.* 21:5097–5108.

Bian, D., S. Su, C. Mahanivong, R.K. Cheng, Q. Han, Z.K. Pan, P. Sun, and S. Huang. 2004. Lysophosphatidic acid stimulates ovarian cancer cell migration via a Ras-MEK Kinase 1 pathway. *Cancer Res.* 64:4209–4217.

Brown, R.A., and P.R. Shepherd. 2001. Growth factor regulation of the novel class II phosphoinositide 3-kinases. *Biochem. Soc. Trans.* 29:535–537.

Brown, R.A., J. Domin, A. Arcaro, M.D. Waterfield, and P.R. Shepherd. 1999. Insulin activates the alpha isoform of class II phosphoinositide 3-kinase. *J. Biol. Chem.* 274:14529–14532.

Cantley, L.C. 2002. The phosphoinositide 3-kinase pathway. *Science.* 296: 1655–1657.

Chaussade, C., L. Pirola, S. Bonnafous, F. Blondeau, S. Brenz-Verca, H. Tronchere, F. Portis, S. Rusconi, B. Payrastre, J. Laporte, and E. Van Obberghen. 2003. Expression of myotubularin by an adenoviral vector demonstrates its function as a phosphatidylinositol 3-phosphate [PtdIns(3)P] phosphatase in muscle cell lines: involvement of PtdIns(3)P in insulin-stimulated glucose transport. *Mol. Endocrinol.* 17:2448–2460.

Elbashir, S.M., J. Harborth, K. Weber, and T. Tuschl. 2002. Analysis of gene function in somatic mammalian cells using small interfering RNAs. *Methods.* 26:199–213.

Foster, F.M., C.J. Traer, S.M. Abraham, and M.J. Fry. 2003. The phosphoinositide (PI) 3-kinase family. *J. Cell Sci.* 116:3037–3040.

Gaidarov, I., M.E. Smith, J. Domin, and J.H. Keen. 2001. The class II phosphoinositide 3-kinase C2alpha is activated by clathrin and regulates clathrin-mediated membrane trafficking. *Mol. Cell.* 7:443–449.

Gillooly, D.J., I.C. Morrow, M. Lindsay, R. Gould, N.J. Bryant, J.M. Gaullier, R.G. Parton, and H. Stenmark. 2000. Localization of phosphatidylinositol 3-phosphate in yeast and mammalian cells. *EMBO J.* 19:4577–4588.

Graler, M.H., and E.J. Goetzl. 2002. Lysophospholipids and their G protein-coupled receptors in inflammation and immunity. *Biochim. Biophys. Acta.* 1582:168–174.

Gschwind, A., S. Hart, O.M. Fischer, and A. Ullrich. 2003. TACE cleavage of proamphiregulin regulates GPCR-induced proliferation and motility of cancer cells. *EMBO J.* 22:2411–2421.

Hama, K., J. Aoki, M. Fukaya, Y. Kishi, T. Sakai, R. Suzuki, H. Ohta, T. Yamori, M. Watanabe, J. Chun, and H. Arai. 2004. Lysophosphatidic acid and autotaxin stimulate cell motility of neoplastic and non-neoplastic cells through LPA1. *J. Biol. Chem.* 279:17634–17639.

Holen, T., M. Amarzguioui, M. Wiiger, E. Babaie, and H. Prydz. 2002. Positional effects of short interfering RNAs targeting the human coagulation trigger Tissue Factor. *Nucleic Acids Res.* 30:1757–1766.

Jung, I.D., J. Lee, K.B. Lee, C.G. Park, Y.K. Kim, D.W. Seo, D. Park, H.W. Lee, J.W. Han, and H.Y. Lee. 2004. Activation of p21-activated kinase 1 is required for lysophosphatidic acid-induced focal adhesion kinase phosphorylation and cell motility in human melanoma A2058 cells. *Eur. J. Biochem.* 271:1557–1565.

Kamalati, T., H.E. Jolin, M.J. Fry, and M.R. Crompton. 2000. Expression of the BRK tyrosine kinase in mammary epithelial cells enhances the coupling of EGF signaling to PI 3-kinase and Akt, via erbB3 phosphorylation. *Oncogene.* 19:5471–5476.

Katso, R., K. Okkenhaug, K. Ahmadi, S. White, J. Timms, and M.D. Waterfield. 2001. Cellular function of phosphoinositide 3-kinases: implications for development, homeostasis and cancer. *Annu. Rev. Cell Dev. Biol.* 17:615–675.

Laffargue, M., P. Raynal, A. Yart, C. Peres, R. Wetzker, S. Roche, B. Payrastre, and H. Chap. 1999. An epidermal growth factor receptor/Gab1 signaling pathway is required for activation of phosphoinositide 3-kinase by lysophosphatidic acid. *J. Biol. Chem.* 274:32835–32841.

Laporte, J., F. Blondeau, A. Gansmuller, Y. Lutz, and J.-L. Vonesch. 2002. The PtdIns3P phosphatase myotubularin is a cytoplasmic protein that also localizes to Rac1-inducible plasma membrane ruffles. *J. Cell Sci.* 115:3105–3117.

Maffucci, T., A. Brancaccio, E. Piccolo, R.C. Stein, and M. Falasca. 2003. Insulin induces phosphatidylinositol-3-phosphate formation through TC10 activation. *EMBO J.* 22:4178–4189.

Mills, G.B., and W.H. Moolenaar. 2003. The emerging role of lysophosphatidic acid in cancer. *Nat. Rev. Cancer.* 3:582–591.

Moolenaar, W.H. 1994. LPA: a novel lipid mediator with diverse biological actions. *Trends Cell Biol.* 4:213–219.

Piccolo, E., S. Vignati, T. Maffucci, P.F. Innominato, A.M. Riley, B.V. Potter, P.P. Pandolfi, M. Broggini, S. Iacobelli, P. Innocenti, and M. Falasca. 2004. Inositol pentakisphosphate promotes apoptosis through a PI 3-K/Akt pathway. *Oncogene.* 23:1754–1765.

Radeff-Huang, J., T.M. Seasholtz, R.G. Matteo, and J.H. Brown. 2004. G protein mediated signaling pathways in lysophospholipid induced cell proliferation and survival. *J. Cell. Biochem.* 92:949–966.

Rameh, L.E., and L.C. Cantley. 1999. The role of phosphoinositide 3-kinase lipid products in cell function. *J. Biol. Chem.* 274:8347–8350.

Razzini, G., A. Brancaccio, M.A. Lemmon, S. Guarnieri, and M. Falasca. 2000. The role of the pleckstrin homology domain in membrane targeting and activation of phospholipase Cbeta(1). *J. Biol. Chem.* 275:14873–14881.

Splinter, P., A.I. Masyuk, and N.F. LaRusso. 2003. Specific inhibition of AQP1 water channels in isolated rat intrahepatic bile duct units by small interfering RNAs. *J. Biol. Chem.* 278:6268–6274.

Stahle, M., C. Veit, U. Bachfischer, K. Schierling, B. Skripczynski, A. Hall, P. Gierschik, and K. Giehl. 2003. Mechanisms in LPA-induced tumor cell migration: critical role of phosphorylated ERK. *J. Cell Sci.* 116:3835–3846.

Stephens, L.R., A. Eguinoa, H. Erdjument-Bromage, M. Lui, F. Cooke, J. Coadwell, A.S. Smrcka, M. Thelen, K. Cadwallader, P. Tempst, and P.T. Hawkins. 1997. The G beta gamma sensitivity of a PI3K is dependent upon a tightly associated adaptor, p101. *Cell.* 89:105–114.

Takeda, H., T. Matozaki, T. Takada, T. Noguchi, T. Yamao, M. Tsuda, F. Ochi, K. Fukunaga, K. Inagaki, and M. Kasuga. 1999. PI 3-kinase gamma and protein kinase C-zeta mediate RAS-independent activation of MAP kinase by a Gi protein-coupled receptor. *EMBO J.* 18:386–395.

Turner, S.J., J. Domin, M.D. Waterfield, S.G. Ward, and J. Westwick. 1998. The CC chemokine monocyte chemotactic peptide-1 activates both the class I p85/p110 phosphatidylinositol 3-kinase and the class II PI3K-C2alpha. *J. Biol. Chem.* 273:25987–25995.

Umezu-Goto, M., Y. Kishi, A. Taira, K. Hama, N. Dohmae, K. Takio, T. Yamori, G.B. Mills, K. Inoue, J. Aoki, and H. Arai. 2002. Autotaxin has lysophospholipase D activity leading to tumor cell growth and motility by lysophosphatidic acid production. *J. Cell Biol.* 158:227–233.

van Leeuwen, F.N., B.N. Giepmans, L.A. van Meeteren, and W.H. Moolenaar. 2003. Lysophosphatidic acid: mitogen and motility factor. *Biochem. Soc. Trans.* 31:1209–1212.

Westermann, A.M., E. Havik, F.R. Postma, J.H. Beijnen, O. Dalesio, W.H. Moolenaar, and S. Rodenhuis. 1998. Malignant effusions contain lysophosphatidic acid (LPA)-like activity. *Ann. Oncol.* 9:437–442.

Xie, Y., T.C. Gibbs, Y.V. Mukhin, and K.E. Meier. 2002. Role for 18:1 lysophosphatidic acid as an autocrine mediator in prostate cancer cells. *J. Biol. Chem.* 277:32516–32526.

Xu, Y., D.C. Gaudette, J.D. Boynton, A. Frankel, X.J. Fang, A. Sharma, J. Hurteau, G. Casey, A. Goodbody, A. Mellors, et al. 1995. Characterization of an ovarian cancer activating factor in ascites from ovarian cancer patients. *Clin. Cancer Res.* 1:1223–1232.

Yamada, T., K. Sato, M. Komachi, E. Malchinkhuu, M. Tobo, T. Kimura, A. Kuwabara, Y. Yanagita, T. Ikeya, Y. Tanahashi, et al. 2004. Lysophosphatidic acid (LPA) in malignant ascites stimulates motility of human pancreatic cancer cells through LPA1. *J. Biol. Chem.* 279:6595–6605.

Yart, A., H. Chap, and P. Raynal. 2002. Phosphoinositide 3-kinases in lysophosphatidic acid signaling: regulation and cross-talk with the Ras/mitogen-activated protein kinase pathway. *Biochim. Biophys. Acta.* 1582:107–111.

Zhang, J., H. Banfic, F. Straforini, L. Tosi, S. Volinia, and S.E. Rittenhouse. 1998. A type II phosphoinositide 3-kinase is stimulated via activated integrin in platelets. A source of phosphatidylinositol 3-phosphate. *J. Biol. Chem.* 273:14081–14084.